Journal of Materials Chemistry A

REVIEW

View Article Online
View Journal | View Issue

CrossMark click for updates

Cite this: J. Mater. Chem. A, 2015, 3, 4765

Benzo[1,2-*b*:4,5-*b*′]dithiophene (BDT)-based small molecules for solution processed organic solar cells

Miaomiao Li, Wang Ni, Xiangjian Wan,* Qian Zhang, Bin Kan and Yongsheng Chen*

Received 25th November 2014
Accepted 7th January 2015

DOI: 10.1039/c4ta06452f

www.rsc.org/MaterialsA

Solution processed small molecule based solar cells have become a competitive alternative to their polymer counterparts due to the advantages of their defined structure and thus less batch to batch variation. With a large and rigid planar conjugated structure, the benzo[1,2-*b*:4,5-*b*′]dithiophene (BDT) unit has become one of the most widely used and studied building blocks for high performance small molecule based photovoltaic devices. In this review article, we review the progress made in the field of small molecules containing BDT units for solution-processed organic photovoltaic cells. Insights into several important aspects regarding the design and synthesis of BDT based small molecules are also included.

Published on 08 January 2015. Downloaded by Nankai University on 14/03/2015 11:39:46.

Introduction

Solution-processed organic photovoltaic cells (OPVs) have attracted considerable attention recently because of their potential as a promising next-generation green technology with the advantages of solution processability, low cost, lightweight, and flexibility.[1–5] In the past few years, power conversion efficiencies (PCEs) over 9% have been achieved for OPVs based on conjugated polymers as electron donor materials.[6–11] Meanwhile, solution processed small molecule based OPVs (SM-OPVs) are emerging as a competitive alterative to their polymer counterparts due to several important advantages of small molecules, such as well defined structures and therefore less batch to batch variation, easier band structure control, *etc.* To date, state-of-the-art solution processed SM-OPVs have demonstrated PCEs exceeding 9%,[12–15] which is closing the performance gap with the best polymer based OPVs (P-OPVs) and may demonstrate even more potential for OPV technologies.

Similar to that of P-OPVs, the rapid development of SM-OPVs in recent years has been accompanied by innovations of donor molecules. Among various small molecules designed for solution processed solar cells, molecules incorporating with benzo[1,2-*b*:4,5-*b*′]dithiophene (BDT) building blocks have been emerging with good OPV performance. BDT, as an attractive donor building block for donor molecules in OPVs, was chosen for the following reasons. First, its structural symmetry and the rigid fused aromatic system could enhance electron delocalization and promote cofacial π–π stacking in the solid state, thus benefiting charge transport in the devices.[16–18] Second, as a

Key Laboratory of Functional Polymer Materials, Center for Nanoscale Science and Technology, Institute of Polymer Chemistry, College of Chemistry, Collaborative Innovation Center of Chemical Science and Engineering (Tianjin), Nankai University, Tianjin 300071, China. E-mail: xjwan@nankai.edu.cn; yschen99@nankai.edu.cn

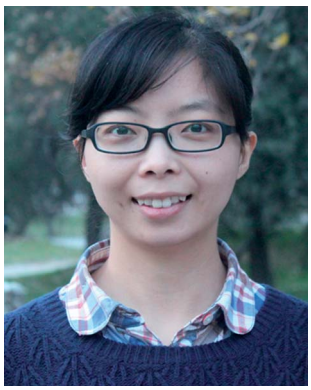

Miaomiao Li received her B.S in Chemistry from Lanzhou University, China, in 2011. She is currently a PhD student at the College of Chemistry, Nankai University. Her PhD research focus is on the fabrication and optimization of small molecule based organic solar cells.

Wang Ni received his B.S in Chemical Engineering and Technology from Tianjin University, China, in 2011. He is currently a PhD student at the College of Chemistry, Nankai University. His PhD research focus is on the design and synthesis of small molecules for organic solar cells.

Published on 08 January 2015. Downloaded by Nankai University on 14/03/2015 11:39:46.

relatively weak donor, BDT would maintain a low highest occupied molecular orbital (HOMO) energy level of the resulting molecules.[19,20] It is to note that currently P-OPVs reported with the highest performances are based on BDT containing polymers.[6–9,21] Currently, solution processed small molecules incorporating BDT units have achieved PCEs near 10%.[13,14]

Several comprehensive reviews have covered the design and synthesis of small molecules including donors and acceptors for vacuum or solution processed OPV devices.[22–24] In this review, we will focus on small molecules employing BDT as the building block for solution processed SM-OPVs. For clarity, BDT-based small molecules are classified into two categories according to the dimension of the conjugated plane of the BDT unit, *i.e.* one-dimensional (1D) and two-dimensional (2D) BDT units. In the first part, one-dimensional BDT based small molecules as donors for SM-OPVs will be described, followed by the discussion of 2D BDT based molecules. BDT based small molecules as acceptors will be presented in the third part. Last part is the Summary and outlook.

One-dimensional BDT (1D BDT) based small molecule donors

In 2011, our group introduced BDT as the central building block to synthesize molecule **1** based on the design strategy of our series of oligothiophene small molecules.[18] The BDT central building block and alkyl cyanoacetate units were linked by trioctylterthiophene π-conjugated spacers to ensure good solubility and also to form an effectively long conjugated acceptor–donor–acceptor (A–D–A) backbone structure with strong intramolecular charge transfer and thus strong and broad absorption. Its film absorption spectrum showed an obvious broadening and bathochromic shift (85 nm) compared to its solution spectrum, and maximum absorption at 563 nm with a shoulder peak at longer wavelength. The blend film of molecule **1** and [6,6]-phenyl-C_{61}-butyric acid methyl ester ($PC_{61}BM$) showed balanced electron and hole mobilities and nanoscale interpenetration. Thus, a high PCE of 5.44% with a high V_{oc} of 0.93 V, a J_{sc} of 9.77 mA cm^{-2} and a notable FF of 59.9% was achieved based on the **1**:$PC_{61}BM$ active layer without any special treatment (Fig. 1).

Following this, with the intention of optimization of morphology and absorption, also easy synthesis, we designed and synthesized two molecules **2** and **3** based on molecule **1**.[25] Three changes were made, *i.e.* introducing 2-ethylhexoxy substituted BDT, easier synthesized dioctylterthiophene and 3-ethylrhodanine end groups. Molecule **2** showed maximum absorption peaks at 494 and 560 nm in diluted chloroform solution and the film, respectively. Under optimized conditions, the device based on molecule **2** showed a PCE of 4.56%, with a V_{oc} of 0.95 V, a J_{sc} of 8.00 mA cm^{-2} and a FF of 60.0%. Although having high V_{oc} and FF, the devices based on molecule **2** with

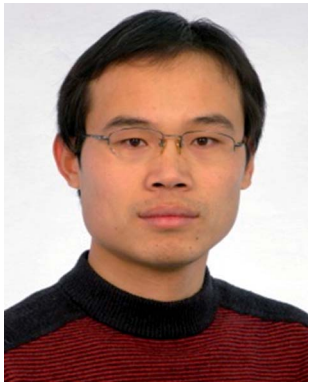

Xiangjian Wan received his PhD degree in Organic Chemistry from Nankai University, China, in 2006. Currently, he is an associate professor of Chemistry, Nankai University. His research interests focus on the organic functional material design and application, especially on solution processed small molecule OPV materials and device optimization.

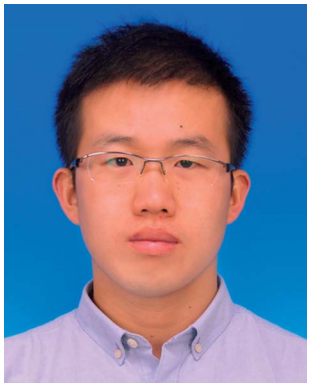

Bin Kan received his B. S in Chemistry from Lanzhou University, China, in 2011. He is currently a PhD student at the College of Chemistry, Nankai University. His PhD research focus is on the design and synthesis of small molecules for organic solar cells.

Qian Zhang received her B. S in Chemistry from Zhenzhou University, China, in 2011. She is currently a PhD student at the College of Chemistry, Nankai University. Her PhD research focus is on the fabrication and optimization of small molecule based organic solar cells.

Prof Yongsheng Chen received his PhD in Chemistry from the University of Victoria in 1997. Since 2003, he has been a Chair Professor at Nankai University. His main research interests focus on carbon-based nanomaterials and organic functional materials for green energy applications.

This journal is © The Royal Society of Chemistry 2015

Published on 08 January 2015. Downloaded by Nankai University on 14/03/2015 11:39:46.

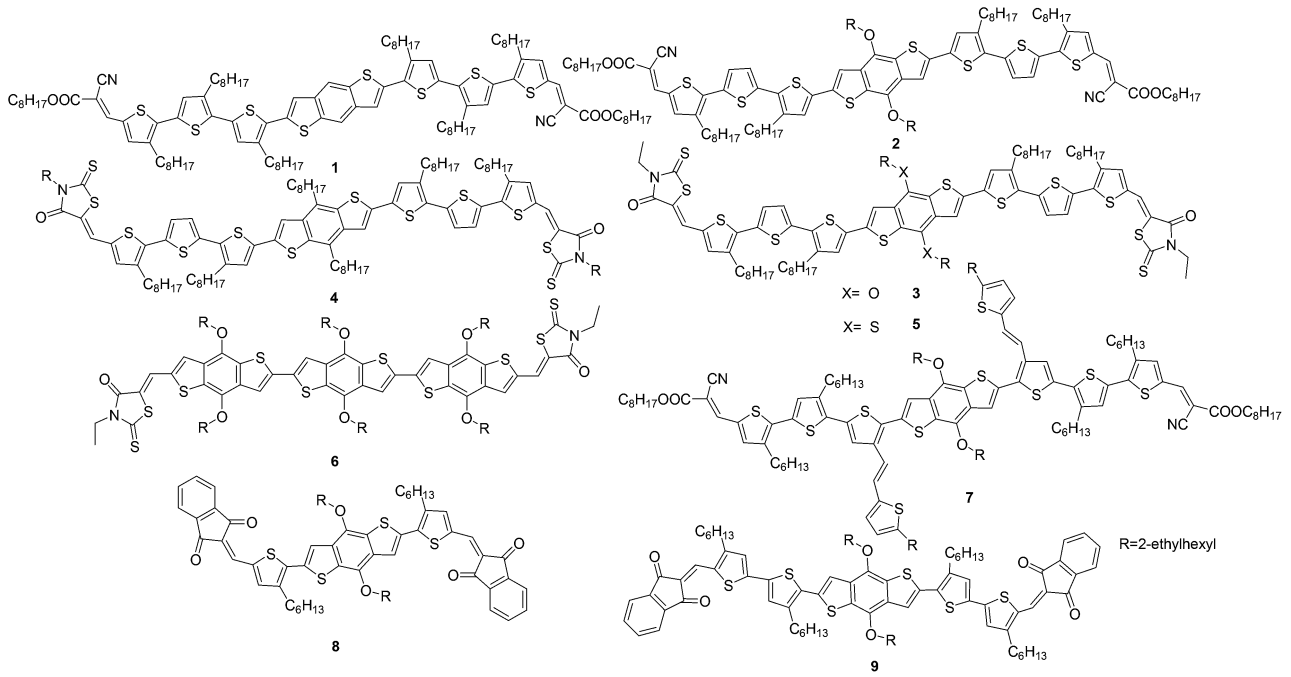

Fig. 1 Molecular structures of **1–9**.

alkyl cyanoacetate as the terminal unit exhibited relatively low J_{sc}. To improve the light absorption ability and thus J_{sc}, a dye unit 3-ethylrhodanine as the end unit was introduced into the molecular design, which was confirmed by our oligothiophene based small molecules. Thus, molecule **3** was designed and synthesized.[25] Compared to **2**, indeed the solution of molecule **3** presented a bathochromic absorption peak at 508 nm with a higher coefficient, and the film showed a broader absorption from 350 to 800 nm and a red-shifted absorption peak at 583 nm and also a vibronic shoulder at 640 nm. The optical band gap of the molecule was 1.74 eV, which was smaller than that of **2**. The OPV device based on molecule **3** and $PC_{71}BM$ exhibited an impressive PCE of 6.92% without any post-treatment. An exciting PCE of 7.38% was achieved with a V_{oc} of 0.93 V, a high J_{sc} of 12.21 mA cm^{-2} and a FF of 65.0% through adding a small amount of polydimethylsiloxane (PDMS) to the active layer. AFM images indicated that the roughness of the active layer film decreased sharply after adding PDMS, which demonstrated more evenly distributed morphological features than that of the film without PDMS. Moreover, it was found from TEM images that with the addition of a small amount of PDMS, the film formed more even continuous interpenetrating networks, and thus it benefited the exciton separation and charge transport and high J_{sc}. Following this work, we reported molecule **4** containing an octyl substituted BDT as the central block.[26] Substituting bulky branched 2-ethylhexyloxy side chains with lower electron-donating octyl chains on BDT was expected to achieve a deeper HOMO energy level and high V_{oc}. Without any special treatment, the OPV device based on the **4**:$PC_{71}BM$ blend film showed an expected higher V_{oc} of 0.98 V compared with that (0.93 V) of molecule **3**. However, the PCE was only 4.34%, with a J_{sc} of 8.52 mA cm^{-2} and a FF of 52%. After both thermal and solvent vapor annealing, the performance was significantly improved resulting in a high PCE of 8.26%, with a V_{oc} of 0.94 V, and a dramatically increased J_{sc} of 12.56 mA cm^{-2} and a FF of 0.70, which were attributed to the much optimized morphology of the photoactive layer indicated by TEM images. After the two step annealing (TSA) treatment, **4**:$PC_{71}BM$ blend films showed a well interpenetrating network with a width of 20 nm, which is comparable to the exciton diffusion length. The results indicate that the simple TSA approach is an efficient strategy to fine tune the morphology of **4**:$PC_{71}BM$ blend films. It is to note that the TSA strategy also does work for **5**:$PC_{71}BM$ based devices. Alkylthio side chains have been employed in organic semiconductors and exhibited some unique optoelectronic properties and more ordered molecular packing.[9,27–29] Recently, we reported small molecule **5**, in which dialkylthiol-substituted BDT was employed as the central building block.[14] Such a little change in the chemical structure led to a great change in the molecular packing behaviour. After TSA treatment mentioned above, the device based on **5**:$PC_{71}BM$ exhibited a PCE as high as 9.95% (certified 9.938%) with a V_{oc} of 0.92 V, a J_{sc} of 14.61 mA cm^{-2} and a notable FF of 74%. The high performance was

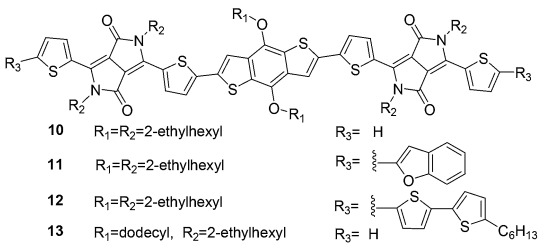

Fig. 2 Molecular structures of **10–13**.

Published on 08 January 2015. Downloaded by Nankai University on 14/03/2015 11:39:46.

Table 1 Photophysical and device performance parameters of **10–13**

SM	E_g^{opt} (eV)	HOMO (eV)	LUMO (eV)	V_{oc} (V)	J_{sc} (mA cm^{-2})	FF	PCE (%)	Ref.
1	1.83	5.11	3.54	0.93	9.77	0.599	5.44	18
2	1.84	5.04	3.24	0.95	8.00	0.60	4.56	25
3	1.74	5.02	3.27	0.93	11.40	0.653	6.92	25
				0.93	12.21	0.650	7.38[a]	25
4	1.79	5.08	3.27	0.98	8.52	0.52	4.34	26
				0.94	12.56	0.70	8.26[b]	26
5	1.74	5.07		0.96	12.32	0.56	6.62	14
				0.92	14.61	0.74	9.95[b]	14
6	1.97	5.34	3.40	0.99	8.26	0.50	4.09	30
7	1.83	5.33	3.44	0.92	6.89	0.63	4.0	31
8	1.59	5.18	3.56	0.91	9.47	0.482	4.15	32
9	1.60	5.16	3.52	0.92	8.58	0.648	5.11	32
10	1.72	5.29	3.57	0.780	8.72	0.444	2.85	33
		5.5	3.7	0.85	8.7	0.51	3.8	34
		5.13	3.65	0.95	3.46	0.41	1.34[d]	37
11	1.60	5.20	3.60	0.800	3.49	0.525	1.46	33
				0.786	6.495	0.404	2.061[c]	33
12	1.55	5.14	3.59	0.670	4.12	0.583	1.62	33
				0.569	10.049	0.486	2.776[c]	33
13	1.71	5.30	3.44	0.80	2.83	0.47	1.05	35
				0.76	5.22	0.55	2.19[d]	35

[a] PDMS was added to the active material solution. [b] The active layer was processed by thermal annealing and solvent vapour annealing. [c] CN was added to the active material solution. [d] DIO was added to the active solution.

attributed to the ordered and fibril structures with a domain size of ~15 nm and a bi-continuous interpenetrating network of the active layer morphology after the two step annealing procedure. The above results indicated that high performance of SM-OPVs could be obtained by the combination of careful molecular design and device optimization.

We also reported an oligobenzodithiophene derivative, molecule **6**, comprising three BDT units end-capped with 3-ethyl-rhodanine.[30] The optical band gap (E_g^{opt}) of molecule **6** was estimated to be 1.97 eV, which was larger than those of the above molecules **1–5**. The three rigid BDT units might not form efficient conjugation in contrast to thiophene and BDT unit conjugation together due to the steric hindrance between BDT units. Under optimized conditions, the device based on the **6**:$PC_{71}BM$ blend film gave a relatively low PCE of 4.09% with a high V_{oc} of 0.99 V, a J_{sc} of 8.26 mA cm^{-2} and a FF of 0.50.

Similar to molecule **2**, Wong and co-workers developed small molecule **7** with oligothiophene as the arm carrying 2-(2-ethylhexyl)thiophene conjugated side chain.[31] With $PC_{71}BM$ as the acceptor, OPV devices based on the molecule showed a PCE of

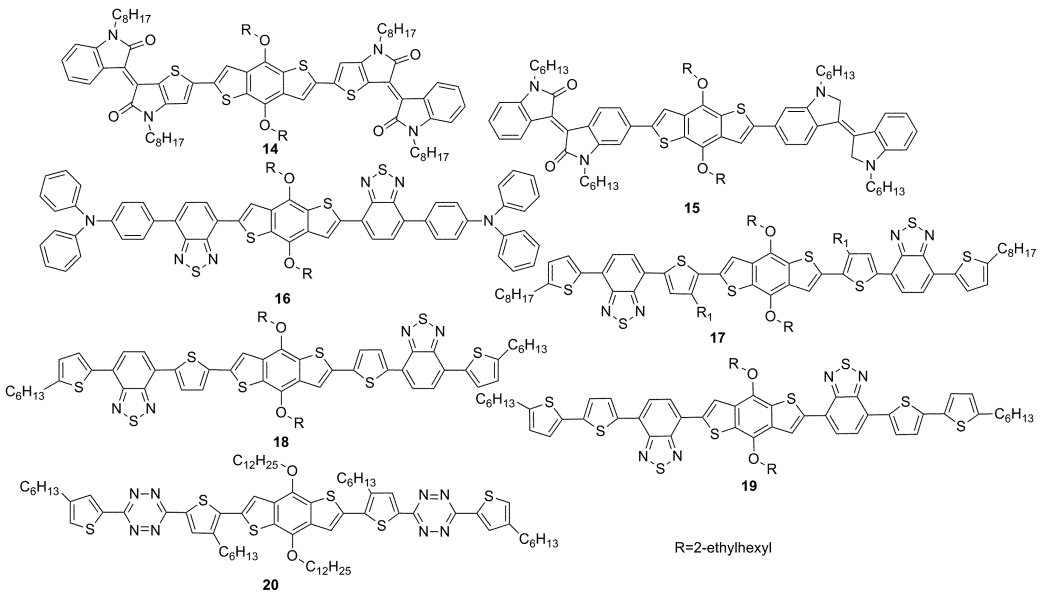

Fig. 3 Molecular structures of **14–20**.

 This journal is © The Royal Society of Chemistry 2015

Published on 08 January 2015. Downloaded by Nankai University on 14/03/2015 11:39:46.

Table 2 Photophysical and device performance parameters of **14–20**

SM	E_g^{opt} (eV)	HOMO (eV)	LUMO (eV)	V_{oc} (V)	J_{sc} (mA cm^{-2})	FF	PCE (%)	Ref.
14	1.68	5.18	3.45	0.72	4.89	0.43	1.51	36
15	1.87	5.25	3.52					36
16	1.90	5.44	3.37	0.83	4.80	0.29	1.18	38
				0.89	7.94	0.40	2.83[a]	38
17	1.81	5.09	3.28	0.70	4.15	0.35	1.01[b]	39
				0.76	1.19	0.31	0.29[c]	39
18	1.77	5.17	3.40	0.89	9.33	0.545	4.53	40
19	1.77	5.11	3.34	0.82	4.74	0.405	1.58	40
20	1.93	5.29	3.55	0.75	1.93	0.54	0.78	41

[a] The active layer was processed by thermal annealing. [b] Donor : PCBM weight ratio = 3 : 1. [c] Donor : PCBM weight ratio = 1 : 1.

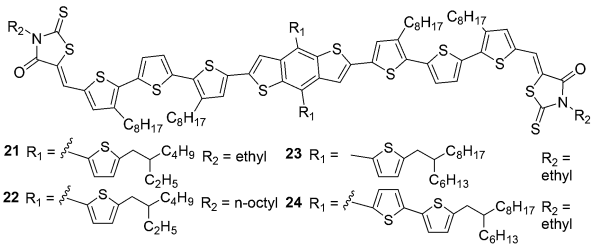

Fig. 4 Molecular structures of **21–24**.

4.0% with a V_{oc} of 0.92 V, a J_{sc} of 6.89 mA cm^{-2}, and a FF of 0.63. Molecules **8** and **9** with indenedione as the acceptor unit and end groups, and thiophene or bithiophene as π-bridges, were designed and synthesized by the Li group for application as donor materials in OPV devices.[32] Molecule **9** with bithiophene π-bridges demonstrated stronger absorbance and higher hole mobility than molecule **8** with thiophene π-bridges. For the two molecules **8** and **9**, the PCEs were 4.15% and 5.11% with a V_{oc} of 0.92 and 0.91 V, a J_{sc} of 8.58 and 9.47 mA cm^{-2}, and a FF of 64.8% and 48.2%, respectively.

Diketopyrrolopyrrole (DPP) is a well known dye unit with many excellent properties such as strong light absorption, photochemical stability, good charge carrier mobility and easy synthesis.[22] Being widely used in P-OPVs, it has drawn great attention in OPV small molecular design. Nguyen *et al.* reported a family of small molecules **10–12** containing BDT as the core and with DPP units in the backbone and with different end-capping groups.[33] The films of the three molecules all showed broad absorption in the visible to near infrared region. Among the three molecules, **10** gave the highest PCE of 2.85% with a V_{oc} of 0.78 V, a J_{sc} of 8.27 mA cm^{-2} and a FF of 44.4%. The molecules **11** and **12** exhibited PCEs of 1.46% and 1.62%, with a V_{oc} of 0.800 V and 0.670 V, a J_{sc} of 3.49 and 4.12 mA cm^{-2}, and a FF of 0.525 and 0.583, respectively. The performance could further be improved by the addition of 2% 1-chloronaphthalene (CN) to the active layer, with PCEs of 2.06% for molecule **11** and 2.776% for molecule **12**. Molecule **10** was also reported by Bisquert *et al.*[34] A higher PCE of 3.8% with a V_{oc} of 0.85 V, a J_{sc} of 8.7 mA cm^{-2} and a FF of 0.51 was obtained owing to the different process of device fabrication. Tu and co-workers also reported a similar molecule **13** with dodecoxy substituted BDT as the core and a PCE of 2.19% was achieved (Fig. 2).[35]

Isoindigo is another attractive dye building block for OPVs. Karakawa and Aso reported molecule **14** using an isoindigo thiophene analogue, in which one of the benzopyrrolidone parts of isoindigo was replaced with thienopyrrolidone.[36] Meanwhile, molecule **15** incorporating an isoindigo unit was also synthesized for comparison.[36] The device with **14** as the donor and $PC_{71}BM$ as the acceptor showed a V_{oc} of 0.72 V, a J_{sc} of 4.89 mA cm^{-2}, and a FF of 0.43, resulting in a PCE of 1.51%. However, the device fabricated from compound **15** did not show any photovoltaic response, which could be due to the poor morphology of the active layer as well as the

Table 3 Photophysical and device performance parameters of **21–24**

SM	E_g^{opt} (eV)	HOMO (eV)	LUMO (eV)	V_{oc} (V)	J_{sc} (mA cm^{-2})	FF	PCE (%)	Ref.
21	1.72	5.02	3.27	0.91	13.15	0.628	7.51	44
				0.93	13.17	0.663	8.12[a]	44
22	1.77	5.5	3.6	0.93	11.4	0.68	7.2	13
				0.94	12.5	0.69	8.1[a]	13
				1.82	7.7	0.72	10.1[b]	13
23	1.76	5.06	3.29	0.96	12.36	0.533	6.32	44
				0.96	11.92	0.594	6.79[a]	44
24	1.76	5.07	3.29	0.90	11.97	0.704	7.58	44
				0.92	12.09	0.721	8.02[a]	44

[a] PDMS was added to the active material solution. [b] The OPV device was a double junction tandem device.

Published on 08 January 2015. Downloaded by Nankai University on 14/03/2015 11:39:46.

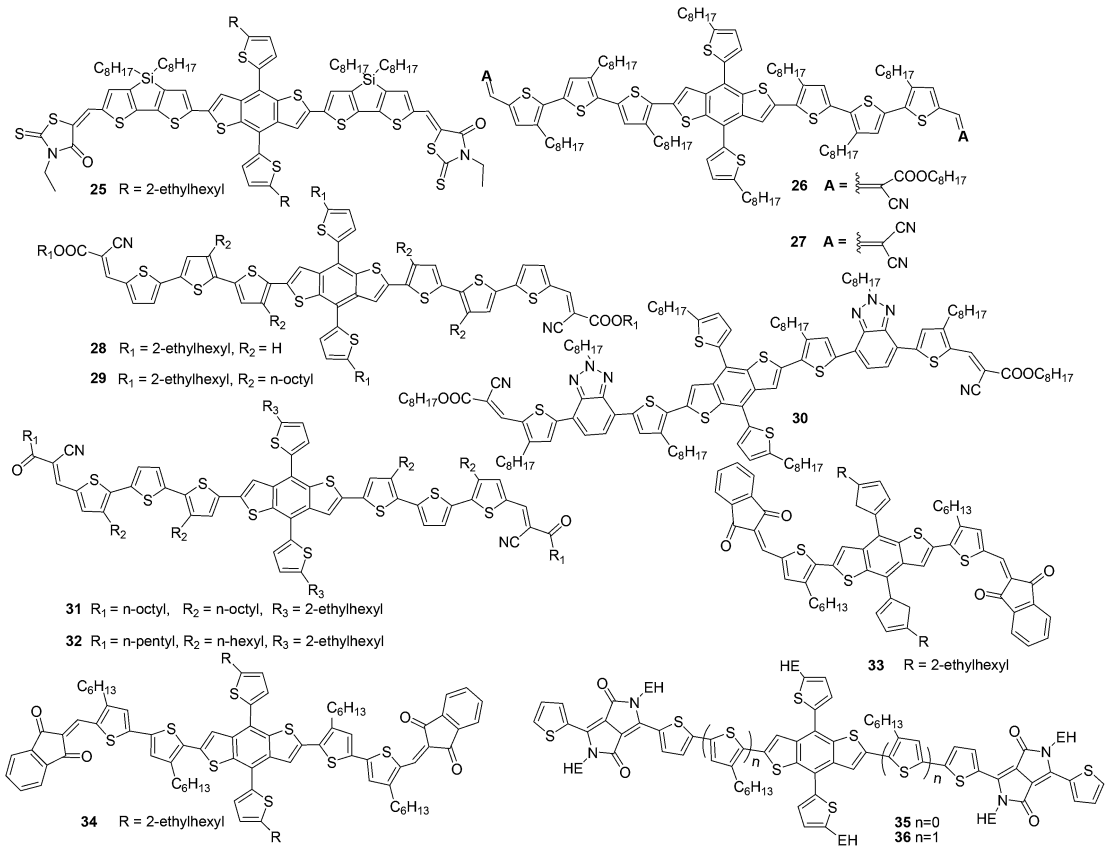

Fig. 5 Molecular structures of **25–36**.

Table 4 Photophysical and device performance parameters of **25–36**

SM	E_g^{opt} (eV)	HOMO (eV)	LUMO (eV)	V_{oc} (V)	J_{sc} (mA cm^{-2})	FF	PCE (%)	Ref.
25	1.82	5.20	3.33	1.022	8.25	0.399	3.36	45
				0.975	10.08	0.513	5.05[a]	45
26	1.75	5.40	3.63	0.90	9.08	0.66	5.42	46
27	1.72	5.45	3.61	0.91	5.17	0.46	2.13	46
28	1.87	5.20	2.90	0.88	6.30	0.75	4.16	47
29	1.80	4.98	2.82	0.97	11.22	0.66	7.19	48
				0.95	11.86	0.70	7.93[a]	48
30	1.85	5.13	3.31	0.93	3.44	0.72	2.31[b]	49
				0.93	5.99	0.64	3.61[c]	49
31	1.76	5.19	3.46	0.93	4.85	0.66	2.99	50
				0.94	8.0	0.70	5.26[d]	50
32	1.77	5.11	3.37	0.89	6.51	0.67	3.88	50
				0.87	9.94	0.65	5.64[d]	50
33	1.61	5.19	3.56	1.03	10.07	0.547	5.67	32
34	1.60	5.16	3.54	0.92	11.05	0.664	6.75	32
35	1.64	5.15	3.44	0.84	6.86	0.43	2.47[e]	51
				0.73	8.63	0.56	3.53[f]	51
				0.72	11.86	0.62	5.29[d]	51
	1.65	5.23	3.46	0.84	11.97	0.576	5.79[a]	52
		5.15	3.44	0.92	4.66	0.47	2.01[d]	37
36		5.20	3.64	0.83	4.60	0.43	1.62[d]	37

[a] The active layer was processed by thermal annealing. [b] Donor : PCBM weight ratio = 1 : 1.5. [c] Donor : PCBM weight ratio = 1 : 1. [d] DIO was added to the active solution. [e] CF as the solvent. [f] *o*-DCB as the solvent.

 This journal is © The Royal Society of Chemistry 2015

Published on 08 January 2015. Downloaded by Nankai University on 14/03/2015 11:39:46.

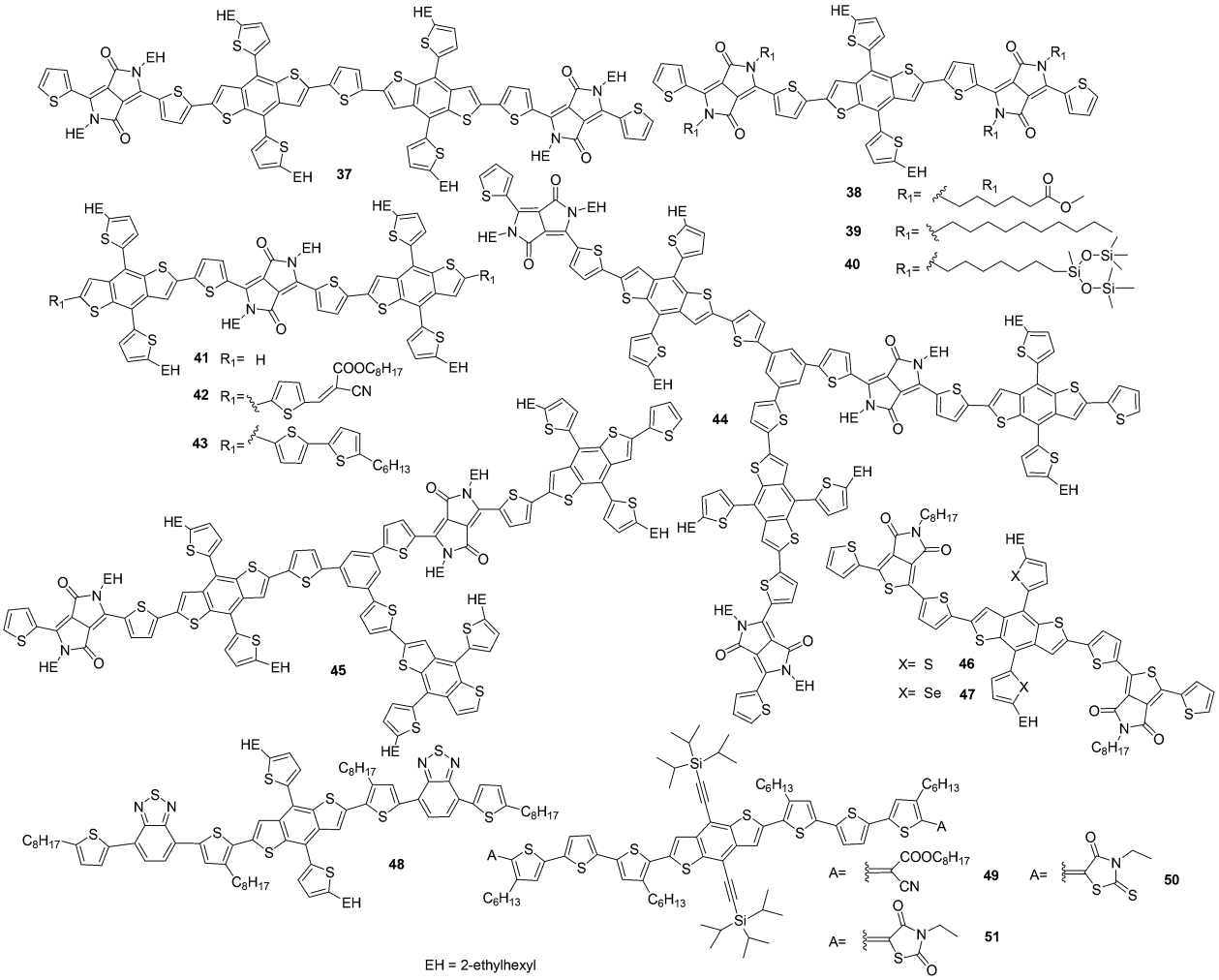

Fig. 6 Molecular structures of **37–51**.

low offset value between the LUMO energy levels of **15** and $PC_{61}BM$ (Table 1).

Lee *et al.* reported molecule **16**.[38] The molecule was comprised of BDT and benzothiadiazole (BT) units, and triphenylamine was combined with the BT unit in order to take advantage of its good electron-donating and hole-transporting properties, as well as its three-dimensional propeller structure. The film of small molecule **16** showed an absorption band in the range of 300–700 nm with an absorption edge at 650 nm and an optical band gap of 1.90 eV. The device with **16**:$PC_{71}BM$ showed a PCE of 1.18% with a V_{oc} of 0.83 V, a J_{sc} of 4.80 mA cm^{-2}, and a FF of 0.29. By 180 °C thermal annealing, the PCE increased to 2.83% with a V_{oc} of 0.89 V, a J_{sc} of 7.94 mA cm^{-2} and a FF of 0.40, due to a well-organized assembly and improved crystallinity in the molecular film (Fig. 3).

Another BDT-based small molecule **17** with BT units was synthesized by Yang and co-workers.[39] The OPV devices were optimized using $PC_{61}BM$ in a 3 : 1 weight ratio and provided V_{oc} of 0.70 V, J_{sc} of 4.15 mA cm^{-2} and FF of 0.35, resulting in a PCE of 1.01%. For the purpose of understanding the impact of the moiety sequence in the chemical structure of small molecules, the Li group synthesized two isomeric compounds, **18** and **19**, with different sequences of BT and thiophene units.[40] In the chlorobenzene solutions, the intramolecular charge transfer (ICT) absorption band of **18** and **19** appeared at 526 and 569 nm, respectively. In the film state, there are a red-shifted ICT absorption band centred at 596 nm for **18**, and two absorption peaks at 573 and 615 nm for **19**, respectively. Molecule **19** showed a low PCE of 1.58%. However, **18** exhibited a much better OPV performance with a PCE of 4.53%, attributed to the ordered crystalline structure in the blend film with $PC_{61}BM$, and a higher hole mobility (Table 2).

Tu and co-workers developed molecule **20** with tetrazine (Tz) as the electron-accepting moiety, due to the very high electron affinity of Tz.[41] The molecular solution displayed a maximum absorption peak at 407 nm and a vibronic shoulder at 466 nm, implying a more ordered arrangement of the molecules in solution. As a result, the **20**:$PC_{61}BM$ based photovoltaic device exhibited a PCE of 0.78% with a V_{oc} of 0.75 V, a J_{sc} of 1.93 mA cm^{-2} and a FF of 0.54. The low PCE could be attributed to the poor morphology of the active layer.

Published on 08 January 2015. Downloaded by Nankai University on 14/03/2015 11:39:46.

Table 5 Photophysical and device performance parameters of **37–51**

SM	E_g^{opt} (eV)	HOMO (eV)	LUMO (eV)	V_{oc} (V)	J_{sc} (mA cm^{-2})	FF	PCE (%)	Ref.
37	1.72	5.16	3.44	0.83	3.79	0.51	1.62[a]	53
38	1.66	5.15	3.45	0.74	9.32	0.546	3.76	54
39	1.69	5.15	3.45	0.73	4.62	0.549	1.83	54
40	1.69	5.15	3.45	0.64	0.45	0.424	0.12	54
41	1.58	5.16	3.60	0.78	4.22	0.27	0.91	55
42	1.53	5.17	3.67	0.78	3.44	0.57	1.52[a]	55
43	1.55	5.13	3.58	0.64	9.66	0.46	2.85[a]	55
44	1.77	5.13	3.57	0.83	6.78	0.403	2.27	56
				0.72	9.11	0.477	3.13[a,b]	56
				0.77	7.69	0.590	3.60[a]	56
45	1.76	5.14	3.60	0.74	5.57	0.453	1.86	56
46	1.97	5.36	3.39	0.87	7.9	0.566	3.90	57
				0.97	9.1	0.520	4.62[b]	57
47	1.86	5.34	3.48	0.90	10.5	0.463	4.37	58
48	1.81	5.13	3.33	0.89	2.07	0.29	0.54[c]	39
				0.88	1.63	0.29	0.43[d]	39
49	2.14	5.15	3.00	0.99	6.63	0.51	3.35	59
				0.96	10.32	0.59	5.84[e]	59
50	2.09	5.15	3.06	1.02	6.75	0.34	2.36	59
				0.97	8.67	0.60	5.03[a]	59
51	2.21	5.12	2.91	1.00	6.3	0.38	2.40	59
				0.97	8.91	0.62	5.31[a]	59

[a] DIO was added to the active solution. [b] The active layer was processed by thermal annealing. [c] Donor : PCBM weight ratio = 1 : 2. [d] Donor : PCBM weight ratio = 1 : 1. [e] CN was added to the active solution.

Two-dimensional BDT (2D BDT) based small molecule donors

For 1D BDT units substituted with non-conjugated side groups, the π-electrons can only delocalize on their conjugated skeleton. In contrast, for 2D BDT introducing thiophene or other π conjugated groups in the orthogonal direction of BDT, the π-electrons could delocalize to the conjugated side groups resulting in enlarged π-conjugation and thus better interchain π–π stacking, which may be beneficial to exciton diffusion and charge transport. Therefore, great attention has been focused on the design and synthesis of 2D BDT-based OPV materials including polymers and small molecules in recent years.[13,42–44]

In 2013, our group introduced thiophene or bithiophene units at the 4- and 8- positions of the BDT unit of molecule **3** to synthesize 2D BDT molecules **21**, **23** and **24**, in order to achieve a higher J_{sc}.[44] Compared with **3**, the above three molecules with 2D BDT cores showed slight red shifts in both the solution and solid film UV-vis absorption spectra. The film spectra exhibited broad absorption over the range of 300 to 800 nm and the optical band gaps were estimated to be 1.72, 1.76, and 1.76 eV for **21**, **23** and **24**, respectively. The OPV devices were fabricated using $PC_{71}BM$ as the acceptor material. Before the addition of PDMS, **21** and **24** with 2D BDT yielded higher PCEs of 7.51% and 7.58%, with a V_{oc} of 0.91 and 0.90 V, a J_{sc} of 13.15 and 11.97 mA cm^{-2}, and a FF of 62.8% and 70.4%, respectively. The results demonstrated that replacing the central 1D BDT unit in **3** with the 2D BDT unit indeed improved the J_{sc} without sacrificing the V_{oc} and FF. Molecule **24** with two thiophene units at both the 4- and 8- positions of the BDT demonstrated the highest FF among the three compounds, which could be attributed to its high and balanced charge mobilities and good morphology. Molecule **23**, with a bulkier long alkyl chain on the thiophene units at the BDT 4- and 8-positions, resulted in a relatively low PCE of 6.32%, because of the lower mobility and

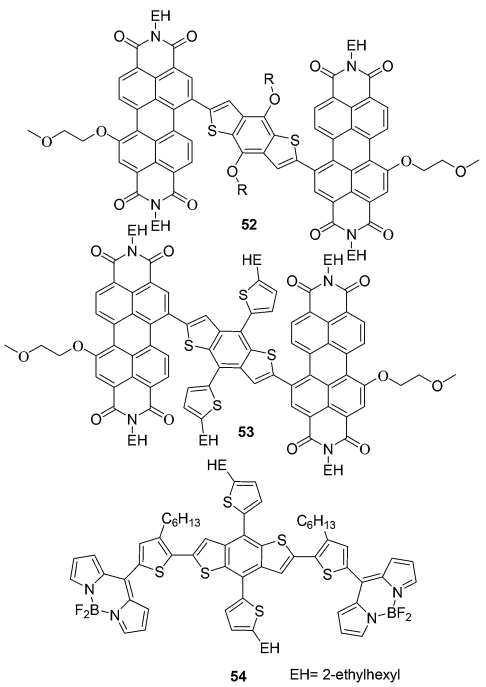

Fig. 7 Molecular structures of **52–54**.

 This journal is © The Royal Society of Chemistry 2015

Published on 08 January 2015. Downloaded by Nankai University on 14/03/2015 11:39:46.

Table 6 Photophysical and device performance parameters of **52–54**

SM	E_g^{opt} (eV)	HOMO (eV)	LUMO (eV)	V_{oc} (V)	J_{sc} (mA cm^{-2})	FF	PCE (%)	Ref.
52	—	5.48	3.84	0.57	0.20	0.261	0.03	60
53	—	5.48	3.84	0.68	5.83	0.490	1.95	60
54	1.73	5.40	3.79	0.65	3.09	0.60	1.21	61

relatively poor morphology. After the addition of PDMS, the PCEs of **21**, **23** and **24** increased to 8.12%, 6.79%, and 8.02%, respectively. The Yang group reported molecule **22**, which has the same chemical structure as that of **21** except for the alkyl chain on the rhodanine unit (Fig. 4).[13] For the device with **22**:$PC_{71}BM$, a PCE of 7.2% was obtained, and was further improved to 8.1%, with a V_{oc} of 0.94 V, a J_{sc} of 12.5 mA cm^{-2}, and a FF of 69%, by adding PDMS to the blend solution. Tandem solar cells comprising two identical photoactive layers as subcells based on **22**:$PC_{71}BM$ were also fabricated. The optimized tandem solar cell achieved a PCE of 10.1%, with a V_{oc} of 1.82 V, a J_{sc} of 7.70 mA cm^{-2}, and a notable FF of 72% (Table 3).

Afterwards, we replaced the trioctylterthiophene of molecule **21** with dithieno[3,2-*b*:20,30-*d*]silole (DTS), and synthesized molecule **25**.[45] The molecule had an absorption peak at 589 nm in solution, and two peaks at 582 and 633 nm in the film. With $PC_{71}BM$ as the acceptor, it yielded a PCE of 3.36%. After annealing at 80 °C for 10 min, an increased PCE of 5.05% was achieved, with a V_{oc} of 0.975 V, a J_{sc} of 10.08 mA cm^{-2} and a FF of 0.513. Morphological analysis from TEM indicated that large aggregation with domain size over 40 nm occurred in the active layer, which was the main factor for the moderate performance.

A series of molecules **26–32** with similar backbones to molecules **21–23**, except for the terminal unit and alkyl chains on the backbone thiophene unit have been designed and synthesized.[46–50] The Chu group designed and synthesized **26** and **27**, end-capped with electron-deficient cyanoacetate (CA) or dicyanovinyl (CN) units.[46] **26** and **27** exhibited optical band gaps with values of 1.72 and 1.75 eV, respectively, which were comparable with those of molecules **21–23**. The device with **26**:$PC_{61}BM$ yielded a PCE of 5.42% with a V_{oc} of 0.90 V, a J_{sc} of 9.08 mA cm^{-2} and a FF of 0.66, whereas the device using **27**:$PC_{61}BM$ exhibited a relatively low PCE of 2.13%, with values of V_{oc},J_{sc}, and FF of 0.91 V, 5.17 mA cm^{-2}, and 0.46, respectively. The higher performance of **26** was attributed to its high miscibility with $PC_{61}BM$ and good π–π stacking ability, which facilitated nanoscale phase separation and enhanced the charge transport and the carrier collection efficiency. Zhan *et al.* reported molecule **28**, in which there were no alkyl chains on the oligothiophene π bridges.[47] The molecule showed a high melting point of 255 °C, a highly ordered assembly of the linear π-conjugated molecule in the solid state, and a hole mobility of 0.01 cm^2 V^{-1} s^{-1}.[47] The solution processed bilayer solar cells based on molecule **28**/$PC_{61}BM$ exhibited a PCE of 4.16%, with an excellent FF up to 0.75, which was attributed to the improved planarity, strong intermolecular interactions and ordered alignment of the molecule. Recently, Yang's group reported molecule **29** with two octyl chains on each oligothiophene π bridge.[48] The OPV device using **29**:$PC_{61}BM$ exhibited a PCE of 7.93%, with a V_{oc} of 0.95 V, a J_{sc} of 11.86 mA cm^{-2} and a FF of 0.70 through a thermal annealing process at 60 °C. The good performance was ascribed to the high crystallinity of **29** in the solid thin film, which could be beneficial for the diffusion of the exciton, and the transport and collection of the carrier. They also replaced the core thiophene of trithiophene in **29** with benzotriazole, and reported **30**.[49] The UV-vis optical spectrum of **30** in chloroform presented an absorption peak at 519 nm and exhibited a maximum absorption peak at 556 nm and a vibronic shoulder peak at 608 nm in the film. The solar cells showed a PCE of 2.31% with a high FF up to 72% at a D/A ratio of 1 : 1.5, and the optimized PCE was 3.61% at a D/A ratio of 1 : 1. Recently, Wei *et al.* reported two molecules **31** and **32** with oxo-alkylated nitrile as the acceptor unit.[50] The two molecules presented similar absorption spectra with the maximum absorption at 504 and 585 nm in solution and in the films, respectively. In the films, a strong shoulder peak (*ca.* 620 nm) at longer wavelengths was observed in both the molecules. The OPV devices fabricated with **31** and **32** showed PCEs of 2.99% and 3.88% without any additives. After the addition of 0.25% DIO (v/v), PCEs of **31** and **32** increased to 5.26% and 5.64%, with a V_{oc} of 0.94 and 0.87 V, a J_{sc} of 8.0 and 9.94 mA cm^{-2}, and a FF of 0.70 and 0.65, respectively. The device with molecule **32** yielded a relatively high J_{sc} compared to that of **31**, because molecule **32** substituted by shorter alkyl chains showed tighter molecular stacking and better ordered crystalline domains in the active layer blend film.

As analogues of molecules **7** and **8**, two molecules **33** and **34** with 2D BDT as the central building block were also reported by the Li group.[32] Under the optimized conditions, PCEs of the OPVs based on **33** and **34** reached 5.67% and 6.75%, with a V_{oc} of 1.03 and 0.92 V, a J_{sc} of 10.07 and 11.05 mA cm^{-2}, and a FF of 54.7% and 66.4%, respectively. Obviously, the photovoltaic performances of **33** and **34** with conjugated thienyl side chains are better than those of **7** and **8** with alkoxy side chains on the BDT unit.

Recently, Zhan and Yao *et al.* have developed a series of 2D BDT and DPP based small molecules.[37,51–53] Compared with molecule **10**, molecule **35** with 2D BDT as the central donor unit exhibited red shift absorption with a maximum at 624 nm, and an optical bandgap of 1.64 eV.[51] The average hole mobility for films spin-coated from *o*-dichlorobenzene (*o*-DCB) with 0.7% DIO was 4.67×10^{-1} cm^2 V^{-1} s^{-1}, which was among the highest of small molecule donors. **35** and $PC_{71}BM$ based devices fabricated from *o*-DCB showed a higher PCE of 3.53% compared to the device fabricated from CF with a PCE of 2.47%. Moreover, by

Published on 08 January 2015. Downloaded by Nankai University on 14/03/2015 11:39:46.

adding 0.7% DIO to *o*-DCB, the molecule exhibited better performance with a V_{oc} of 0.72 V, a J_{sc} of 11.86 mA cm^{-2}, a FF of 62%, and a PCE of 5.29%. Zhan *et al.* also reported molecule **35**.[52] Similar performance with a PCE of 5.79%, a V_{oc} of 0.84 V, a J_{sc} of 11.97 mA cm^{-2} and a FF of 0.576 was obtained through thermal annealing.[52] Furthermore, the Yao group also reported all small molecule solar cells using **10**, **35** and **36** as donors and a perylene diimide dimer (bis-PDI-T-EG) as the acceptor.[37] **35** based all-small-molecule devices yielded the highest PCE of 2.01% with a V_{oc} of 0.92 V, a J_{sc} of 4.66 mA cm^{-2}, and a FF of 0.47. In contrast, **10** and **36** yielded PCEs of 1.34% and 1.62%, with a V_{oc} of 0.95 and 0.83 V, a J_{sc} of 3.46 and 4.60 mA cm^{-2}, and a FF of 0.41 and 0.43, respectively (Fig. 5). Later, to extend the π-back-bone of molecule **35**, the Yao group incorporated two 2D BDT units between the two DPP moieties and synthesized **37**.[53] The constructed all-small-molecule solar cell using bis-PDI-T-EG as the acceptor and **37** as the donor showed a PCE of 1.62% with a V_{oc} of 0.83 V, a J_{sc} of 3.79 mA cm^{-2} and a FF of 0.51, which were comparable with those of the devices based on the blend of **37** and $PC_{61}BM$ with a PCE of 2.08% (Table 4).

Recently, Zhan and Yao *et al.* chose DPP-BDT-DPP as a model backbone and designed compounds **38–40** with different anchoring groups terminated on the N-substituted alkyl-chain spacer of the DPP units.[54] Changing the anchoring terminals had a minimal impact on the solution absorption spectra, because each molecule contained the same molecular skeleton. **38** with the polar –$COOCH_3$ terminal possessed stronger π–π stacking and higher order in the solid state than that observed for **39** and **40** with the less polar –C_5H_{11} and –CSiO terminals. The device with **38**:$PC_{71}BM$ showed the best performance with a V_{oc} of 0.74 V, a J_{sc} of 9.32 mA cm^{-2}, a FF of 0.546 and a PCE of 3.76%, while molecules **39** and **40** exhibited relatively low PCEs of 1.83% and 0.12%, with a V_{oc} of 0.73 and 0.64 V, a J_{sc} of 4.62 and 0.45 mA cm^{-2}, and a FF of 0.549 and 0.424, respectively. The difference of J_{sc} and thus PCE was associated with difference of the phase size with values of 20, 50 and 250 nm for **38**, **39** and **40**, respectively. In contrast to the above DPP-BDT-DPP molecules, **41–43** with the BDT-DPP-BDT backbone and different end groups showed a lower bandgap with values of 1.58, 1.53 and 1.55 eV, respectively.[55] However, the three molecules showed no improvement in the OPV performances with PCEs of 0.91%, 1.52% and 2.85% for **41–43**, respectively. Molecules **44** and **45** with a phenyl-1,3,5-trithienyl core and BDT-DPP branches were also reported by Zhan and Yao *et al.*[56] A PCE of 3.60% was obtained for the **44**:$PC_{71}BM$ based devices with the DIO additive, whereas **45** exhibited a relatively low PCE of 1.86% owing to its low light-harvesting ability and hole mobility (Fig. 6).

Molecules **46** and **47** composed of 2D BDT as the core building block and thiophene-bridged thieno[3,4-*c*]pyrrole-4,6-dione (TPD) as the acceptor arm unit were reported by Kim and Park *et al.*[57,58] Devices based on **46**:$PC_{61}BM$ showed a PCE of 3.90%, and the PCE increased to 4.62% after thermal annealing at 120 °C.[57] With the introduction of selenophene onto BDT, the film of molecule **47** showed a red-shifted absorption compared with the film of **46**.[58] The PCE of the device based on **47**:$PC_{71}BM$ was 4.37%, with a V_{oc} of 0.90 V, a J_{sc} of 10.5 mA cm^{-2}, and a FF of 46.3%. Molecule **48** containing benzothiadiazole and 2D-BDT yielded a PCE of 0.43%, which was higher than that of **17** with a PCE of 0.29% under the same conditions (donor : $PC_{61}BM$ = 1 : 1).[39]

Ko *et al.* introduced triisopropylsilylethynyl (TIPS) into BDT, and synthesized compounds **49–51**.[59] TIPS was used to extend the π-conjugation and induce a rigid structure, producing a more electron-rich BDT that would facilitate intramolecular charge transfer as well as molecular self-networking. The molecules **49–51** had strong ICT absorption in solution with high maximum extinction coefficients of 111 800 M^{-1} cm^{-1} at 526 nm, 134 000 M^{-1} cm^{-1} at 509 nm and 138 000 M^{-1} cm^{-1} at 500 nm, and deep HOMO levels of 5.15, 5.15 and 5.12 eV, respectively. The conventionally fabricated devices with **49–51** as donors and $PC_{61}BM$ as the acceptor showed PCEs of 3.35%, 2.36% and 2.40%, respectively, with a notably high V_{oc} around 1 V. After device optimization with additive of CN or DIO, PCEs over 5% were achieved for the three molecule based devices, mainly attributed to the improved J_{sc} and FF. The addition of CN and DIO additives with high boiling points to the active layers facilitated intermolecular π–π packing interactions of the semiconducting small molecules in the BHJ films, and the formation of highly phase-segregated morphologies, which resulted in strongly enhanced J_{sc} and FF, and thus significantly improved PCEs (Table 5).

BDT-based materials as acceptors in OPV devices

Some of the BDT-based materials can present low LUMO energy levels and high electron mobilities by connecting with appropriate substituents.[60,61] The properties make these BDT-based materials electronically suitable as acceptors for OPV devices.

Zhan and Yao *et al.* reported molecules **52** and **53** with perylene diimide (PDI) dimers, using 1D-BDT and 2D-BDT as covalent bridges, respectively.[60] The OPV devices were fabricated based on these molecules as the acceptors and poly(3-hexylthiophene) (P3HT) as the donor. **52** showed a poor OPV performance, only with a low PCE of 0.03%, due to its over-strong aggregation, limited solubility (<1 mg ml^{-1}) and very poor solution-processability. However, **53** had good solubility (>20 mg mL^{-1}) and exhibited reduced aggregation ability, which was ascribed to the solvophilic and twisted 4,8-bis-substituted thienyl units at the bridged BDT unit. When molecule **53** was blended with P3HT, a PCE of 1.95% was achieved through slow-speed solvent evaporation.

Thayumanavan *et al.* connected 4,4-difluoro-4-bora-3*a*,4*a*-diaza-*s*-indacene (BODIPY) as the acceptor moiety to the BDT unit, obtaining molecule **54** (Fig. 7).[61] An inverted device using P3HT as the donor material was fabricated, yielding a PCE of 1.21% with a V_{oc} of 0.65, a J_{sc} of 3.09 mA cm^{-2} and a FF of 0.60 (Table 6).

Conclusion and outlook

Solution-processed organic solar cells based on BDT small molecule donors showed good performance attributed to their unique chemical structures and thus good physical properties and ideal morphology forming tendency. BDT units, with their

 This journal is © The Royal Society of Chemistry 2015

Published on 08 January 2015. Downloaded by Nankai University on 14/03/2015 11:39:46.

structural symmetry and rigid fused aromatic system, could enhance the electron delocalization and promote co-facial π–π stacking and crystallization in the solid state, thus benefiting charge transport in the devices. Through delicate molecular design together with device optimization, highly crystalline donor fibrils with a domain size of 10–20 nm comparable to the typical exciton diffusion length could be formed. In addition, as a relatively weak donor unit, BDT would be helpful to maintain a low HOMO energy level for its parent molecules, which is favorable to obtain high V_{oc}. Compared with 1D-BDT-based donor molecules, 2D-BDT donor molecules, with the expanded conjugation area of their backbones, generally showed higher J_{sc} and FF, arising from the improved electron donating capability and hole mobility. Hence, in many cases, the OPV performance of 2D-BDT molecules was superior to that of 1D-BDT-based materials. Furthermore, through the insertion of different electron acceptor parts, the energy levels and bandgap of BDT-based small molecules could be tuned. And by connecting larger π-bridges, BDT analogues can present higher hole mobility and stronger absorption. Tuning the number and length of alkyl groups on the backbone could not only change the solubility of the molecules, but also adjust the packing modes of donor molecules themselves. Beyond molecular design, device optimization, especially morphology optimization, plays an extremely important role in yielding a high PCE. It was demonstrated that many processing procedures can be utilized to adjust and control the morphology and thus to achieve optimized morphology, including adding high-boiling solvents and other suitable additives, conducting thermal annealing or solvent vapor annealing of active layers and combining multiple methods together. The high performance of molecule **5** based devices was realized indeed through the combination of careful molecular design and device optimization. We believe that higher PCEs will be achieved for SM-OPVs through reasonable design of BDT based donor molecules and optimized device fabrication.

Besides, it is worth noting that acceptors containing BDT units have shown promising photovoltaic performances. It would be worthwhile to further functionalize BDT with a greater variety of heterocyclic groups for obtaining high-performance acceptor molecules.

The introduction of BDT moieties has significantly contributed to the development of solution-processed SM-OPVs. The feasible synthesis routes and tunable properties of BDT-based small molecules make them promising materials in SM-OPVs. It is believed that further exploration of BDT-based small molecules will provide a new breakthrough and accelerate the commercial production of SM-OPVs in the near future.

Acknowledgements

The authors gratefully acknowledge the financial support from MoST (2014CB643502), NSFC (51373078 and 51422304), and PCSIRT (IRT1257).

Notes and references

1 A. J. Heeger, *Chem. Soc. Rev.*, 2010, **39**, 2354–2371.
2 D. J. Lipomi and Z. Bao, *Energy Environ. Sci.*, 2011, **4**, 3314–3328.
3 F. He and L. Yu, *J. Phys. Chem. Lett.*, 2011, **2**, 3102–3113.
4 Y. Lin, H. F. Dam, T. R. Andersen, E. Bundgaard, W. Fu, H. Chen, F. C. Krebs and X. Zhan, *J. Mater. Chem. C*, 2013, **1**, 8007–8010.
5 H. Zhou, L. Yang and W. You, *Macromolecules*, 2012, **45**, 607–632.
6 Z. He, C. Zhong, S. Su, M. Xu, H. Wu and Y. Cao, *Nat. Photonics*, 2012, **6**, 591–595.
7 S.-H. Liao, H.-J. Jhuo, Y.-S. Cheng and S.-A. Chen, *Adv. Mater.*, 2013, **25**, 4766–4771.
8 X. Guo, M. Zhang, W. Ma, L. Ye, S. Zhang, S. Liu, H. Ade, F. Huang and J. Hou, *Adv. Mater.*, 2014, **26**, 4043–4049.
9 L. Ye, S. Zhang, W. Zhao, H. Yao and J. Hou, *Chem. Mater.*, 2014, **26**, 3603–3605.
10 T. L. Nguyen, H. Choi, S. J. Ko, M. A. Uddin, B. Walker, S. Yum, J. E. Jeong, M. H. Yun, T. J. Shin, S. Hwang, J. Y. Kim and H. Y. Woo, *Energy Environ. Sci.*, 2014, **7**, 3040–3051.
11 C.-Z. Li, C.-Y. Chang, Y. Zang, H.-X. Ju, C.-C. Chueh, P.-W. Liang, N. Cho, D. S. Ginger and A. K. Y. Jen, *Adv. Mater.*, 2014, **26**, 6262–6267.
12 A. K. K. Kyaw, D. H. Wang, D. Wynands, J. Zhang, T.-Q. Nguyen, G. C. Bazan and A. J. Heeger, *Nano Lett.*, 2013, **13**, 3796–3801.
13 Y. Liu, C.-C. Chen, Z. Hong, J. Gao, Y. Yang, H. Zhou, L. Dou and G. Li, *Sci. Rep.*, 2013, **3**, 3356.
14 B. Kan, Q. Zhang, M. Li, X. Wan, W. Ni, G. Long, Y. Wang, X. Yang, H. Feng and Y. Chen, *J. Am. Chem. Soc.*, 2014, **136**, 15529–15532.
15 Q. Zhang, B. Kan, F. Liu, G. Long, X. Wan, X. Chen, Y. Zuo, W. Ni, H. Zhang, M. Li, Z. Hu, F. Huang, Y. Cao, Z. Liang, M. Zhang, T. P. Russell and Y. Chen, *Nat. Photonics*, 2014, 269, DOI: 10.1038/nphoton.
16 Y. Liang, Y. Wu, D. Feng, S.-T. Tsai, H.-J. Son, G. Li and L. Yu, *J. Am. Chem. Soc.*, 2008, **131**, 56–57.
17 H.-Y. Chen, J. Hou, S. Zhang, Y. Liang, G. Yang, Y. Yang, L. Yu, Y. Wu and G. Li, *Nat. Photonics*, 2009, **3**, 649–653.
18 Y. Liu, X. Wan, F. Wang, J. Zhou, G. Long, J. Tian and Y. Chen, *Adv. Mater.*, 2011, **23**, 5387–5391.
19 H. Zhou, L. Yang, S. C. Price, K. J. Knight and W. You, *Angew. Chem., Int. Ed.*, 2010, **49**, 7992–7995.
20 H. Zhou, L. Yang, S. Stoneking and W. You, *ACS Appl. Mater. Interfaces*, 2010, **2**, 1377–1383.
21 J. Kong, I.-W. Hwang and K. Lee, *Adv. Mater.*, 2014, **26**, 6275–6283.
22 S. Qu and H. Tian, *Chem. Commun.*, 2012, **48**, 3039–3051.
23 Y. Chen, X. Wan and G. Long, *Acc. Chem. Res.*, 2013, **46**, 2645–2655.
24 J. E. Coughlin, Z. B. Henson, G. C. Welch and G. C. Bazan, *Acc. Chem. Res.*, 2013, **47**, 257–270.
25 J. Zhou, X. Wan, Y. Liu, Y. Zuo, Z. Li, G. He, G. Long, W. Ni, C. Li, X. Su and Y. Chen, *J. Am. Chem. Soc.*, 2012, **134**, 16345–16351.
26 W. Ni, M. Li, X. Wan, H. Feng, B. Kan, Y. Zuo and Y. Chen, *RSC Adv.*, 2014, **4**, 31977–31980.

Published on 08 January 2015. Downloaded by Nankai University on 14/03/2015 11:39:46.

27 L. Huo, Y. Zhou and Y. Li, *Macromol. Rapid Commun.*, 2009, **30**, 925–931.
28 K. Li, Z. Li, K. Feng, X. Xu, L. Wang and Q. Peng, *J. Am. Chem. Soc.*, 2013, **135**, 13549–13557.
29 C. Cui, W.-Y. Wong and Y. Li, *Energy Environ. Sci.*, 2014, **7**, 2276–2284.
30 W. Ni, M. Li, X. Wan, Y. Zuo, B. Kan, H. Feng, Q. Zhang and Y. Chen, *Sci. China: Chem.*, DOI: 10.1007/s11426-014-5220-x
31 C. Cui, J. Min, C.-L. Ho, T. Ameri, P. Yang, J. Zhao, C. J. Brabec and W.-Y. Wong, *Chem. Commun.*, 2013, **49**, 4409–4411.
32 S. Shen, P. Jiang, C. He, J. Zhang, P. Shen, Y. Zhang, Y. Yi, Z. Zhang, Z. Li and Y. Li, *Chem. Mater.*, 2013, **25**, 2274–2281.
33 B. Walker, J. Liu, C. Kim, G. C. Welch, J. K. Park, J. Lin, P. Zalar, C. M. Proctor, J. H. Seo, G. C. Bazan and T.-Q. Nguyen, *Energy Environ. Sci.*, 2013, **6**, 952–962.
34 A. Guerrero, S. Loser, G. Garcia-Belmonte, C. J. Bruns, J. Smith, H. Miyauchi, S. I. Stupp, J. Bisquert and T. J. Marks, *Phys. Chem. Chem. Phys.*, 2013, **15**, 16456–16462.
35 C. Li, Y. Chen, Y. Zhao, H. Wang, W. Zhang, Y. Li, X. Yang, C. Ma, L. Chen, X. Zhu and Y. Tu, *Nanoscale*, 2013, **5**, 9536–9540.
36 M. Karakawa and Y. Aso, *RSC Adv.*, 2013, **3**, 16259–16263.
37 J. Huang, X. Wang, X. Zhang, Z. Niu, Z. Lu, B. Jiang, Y. Sun, C. Zhan and J. Yao, *ACS Appl. Mater. Interfaces*, 2014, **6**, 3853–3862.
38 P. Dutta, J. Kim, S. H. Eom, W.-H. Lee, I. N. Kang and S.-H. Lee, *ACS Appl. Mater. Interfaces*, 2012, **4**, 6669–6675.
39 Y. Chen, Y. Yan, Z. Du, X. Bao, Q. Liu, V. A. L. Roy, M. Sun, R. Yang and C. S. Lee, *J. Mater. Chem. C*, 2014, **2**, 3921–3927.
40 L. Liang, J.-T. Wang, X. Xiang, J. Ling, F.-G. Zhao and W.-S. Li, *J. Mater. Chem. A*, 2014, **2**, 15396–15405.
41 P. Zhang, C. Li, Y. Zhao, Y. Li and Y. Tu, *Chin. J. Chem.*, 2013, **31**, 1439–1448.
42 L. Huo, J. Hou, S. Zhang, H.-Y. Chen and Y. Yang, *Angew. Chem., Int. Ed.*, 2010, **49**, 1500–1503.
43 L. Ye, S. Zhang, L. Huo, M. Zhang and J. Hou, *Acc. Chem. Res.*, 2014, **47**, 1595–1603.
44 J. Zhou, Y. Zuo, X. Wan, G. Long, Q. Zhang, W. Ni, Y. Liu, Z. Li, G. He, C. Li, B. Kan, M. Li and Y. Chen, *J. Am. Chem. Soc.*, 2013, **135**, 8484–8487.
45 Z. Yi, W. Ni, Q. Zhang, M. Li, B. Kan, X. Wan and Y. Chen, *J. Mater. Chem. C*, 2014, **2**, 7247–7255.
46 D. Patra, T.-Y. Huang, C.-C. Chiang, R. O. V. Maturana, C.-W. Pao, K.-C. Ho, K.-H. Wei and C.-W. Chu, *ACS Appl. Mater. Interfaces*, 2013, **5**, 9494–9500.
47 Y. Lin, L. Ma, Y. Li, Y. Liu, D. Zhu and X. Zhan, *Adv. Energy Mater.*, 2014, **4**, 1300626.
48 Z. Du, W. Chen, Y. Chen, S. Qiao, X. Bao, S. Wen, M. Sun, L. Han and R. Yang, *J. Mater. Chem. A*, 2014, **2**, 15904–15911.
49 Y. Chen, Z. Du, W. Chen, Q. Liu, L. Sun, M. Sun and R. Yang, *Org. Electron.*, 2014, **15**, 405–413.
50 D. Deng, Y. Zhang, L. Yuan, C. He, K. Lu and Z. Wei, *Adv. Energy Mater.*, 2014, 1400538.
51 J. Huang, C. Zhan, X. Zhang, Y. Zhao, Z. Lu, H. Jia, B. Jiang, J. Ye, S. Zhang, A. Tang, Y. Liu, Q. Pei and J. Yao, *ACS Appl. Mater. Interfaces*, 2013, **5**, 2033–2039.
52 Y. Lin, L. Ma, Y. Li, Y. Liu, D. Zhu and X. Zhan, *Adv. Energy Mater.*, 2013, **3**, 1166–1170.
53 Y. Chen, A. Tang, X. Zhang, Z. Lu, J. Huang, C. Zhan and J. Yao, *J. Mater. Chem. A*, 2014, **2**, 1869–1876.
54 A. Tang, Z. Lu, S. Bai, J. Huang, Y. Chen, Q. Shi, C. Zhan and J. Yao, *Chem.–Asian J.*, 2014, **9**, 883–892.
55 S. Zhang, X. Wang, A. Tang, J. Huang, C. Zhan and J. Yao, *Phys. Chem. Chem. Phys.*, 2014, **16**, 4664–4671.
56 S. Zhang, B. Jiang, C. Zhan, J. Huang, X. Zhang, H. Jia, A. Tang, L. Chen and J. Yao, *Chem.–Asian J.*, 2013, **8**, 2407–2416.
57 J.-j. Ha, Y. J. Kim, J.-g. Park, T. K. An, S.-K. Kwon, C. E. Park and Y.-H. Kim, *Chem.–Asian J.*, 2014, **9**, 1045–1053.
58 Y. J. Kim, J. Y. Baek, J.-j. Ha, D. S. Chung, S.-K. Kwon, C. E. Park and Y.-H. Kim, *J. Mater. Chem. C*, 2014, **2**, 4937–4946.
59 N. Lim, N. Cho, S. Paek, C. Kim, J. K. Lee and J. Ko, *Chem. Mater.*, 2014, **26**, 2283–2288.
60 B. Jiang, X. Zhang, C. Zhan, Z. Lu, J. Huang, X. Ding, S. He and J. Yao, *Polym. Chem.*, 2013, **4**, 4631–4638.
61 A. M. Poe, A. M. Della Pelle, A. V. Subrahmanyam, W. White, G. Wantz and S. Thayumanavan, *Chem. Commun.*, 2014, **50**, 2913–2915.

 This journal is © The Royal Society of Chemistry 2015